LUND UNIVERSITY

# Loss of HIF-1α accelerates murine FLT-3ITD-induced myeloproliferative neoplasia.

Velasco, Talia; Tornero Prieto, Daniel; Cammenga, Jörg

*Published in:*
Leukemia

*DOI:*
10.1038/leu.2015.156

2015

Link to publication

*Citation for published version (APA):*
Velasco, T., Tornero Prieto, D., & Cammenga, J. (2015). Loss of HIF-1α accelerates murine FLT-3ITD-induced myeloproliferative neoplasia. *Leukemia*, *29*(12), 2366-2374. https://doi.org/10.1038/leu.2015.156

*Total number of authors:*
3

**General rights**
Unless other specific re-use rights are stated the following general rights apply:
Copyright and moral rights for the publications made accessible in the public portal are retained by the authors and/or other copyright owners and it is a condition of accessing publications that users recognise and abide by the legal requirements associated with these rights.
• Users may download and print one copy of any publication from the public portal for the purpose of private study or research.
• You may not further distribute the material or use it for any profit-making activity or commercial gain
• You may freely distribute the URL identifying the publication in the public portal

Read more about Creative commons licenses: https://creativecommons.org/licenses/

**Take down policy**
If you believe that this document breaches copyright please contact us providing details, and we will remove access to the work immediately and investigate your claim.

LUND UNIVERSITY

PO Box 117
221 00 Lund
+46 46-222 00 00

Download date: 26. Apr. 2024

# Loss of HIF-1α accelerates murine FLT-3$^{ITD}$-induced myeloproliferative neoplasia

Talia Velasco-Hernandez[1], Daniel Tornero[2] and Jörg Cammenga[1, 3, 4, 5]

[1]Department of Molecular Medicine and Gene Therapy, Lund Stem Cell Center, Lund University, Lund, Sweden; [2]Laboratory of Stem Cells and Restorative Neurology, Lund Stem Cell Center, Skanes University Hospital, Lund, Sweden; [3]Department of Hematology, Skanes University Hospital, Lund, Sweden, [4]Department of Hematology, Linköping University Hospital and [5]Institution for Clinical and Experimental Medicine, Linköping University, Linköping, Sweden.

**Running title:** HIF-1α in FLT-3$^{ITD}$ myeloid neoplasia

**Key words:** Hypoxia, HIF-1α, myeloproliferative neoplasm (MPN), *Flt-3,* tumor suppressor gene.

Correspondence should be addressed to:

Jörg Cammenga

Department of Molecular Medicine and Gene Therapy

Lund Stem Cell Center BMC A12, Sölvegatan 17, 22184 Lund, Sweden

e-mail: jorg.cammenga@med.lu.se

The authors declare no conflict of interests.

**Abstract:**

Hypoxia-induced signaling is important for normal and malignant hematopoiesis. The transcription factor hypoxia-inducible factor-1α (HIF-1α) plays a crucial role in quiescence and self-renewal of hematopoietic stem cells (HSCs) as well as leukemia-initiating cells (LICs) of acute myeloid leukemia (AML) and chronic myeloid leukemia (CML). We have investigated the effect of HIF-1α loss on the phenotype and biology of FLT-$3^{ITD}$-induced myeloproliferative neoplasm (MPN). Using transgenic mouse models, we show that deletion of HIF-1α leads to an enhanced MPN phenotype reflected by higher numbers of white blood cells, more severe splenomegaly and decreased survival. The proliferative effect of HIF-1α loss is cell-intrinsic as shown by transplantation into recipient mice. HSCs loss and organ specific changes in number and percentage of long-term hematopoietic stem cells (LT-HSCs) were the most pronounced effects on a cellular level after HIF-1α deletion. Furthermore, we found a metabolic hyperactivation of malignant cells in the spleen upon loss of HIF-1α. Some of our findings are in contrary to what has been previously described for the role of HIF-1α in other myeloid hematologic malignancies and question the potential of HIF-1α as a therapeutic target.

**Introduction:**

Hypoxia has been proposed to be a physiologic condition in the adult hematopoietic stem cell (HSC) niche and previous publications have provided experimental evidence for this hypothesis[1]. Additionally, it has been shown that hypoxia signaling, through hypoxia-inducible factors (HIFs), is required for proper HSCs function, and that this might be mediated by HIF-induced pyruvate dehydrogenase kinase (PDK) and vascular endothelial growth factor (VEGF) expression[2-4]. Further dissection of the HIF signaling pathway has indicated that HIF-1α, but not HIF-2α, seems to be the major player in HSCs self-renewal[5]. Interestingly, deletion of both members of the HIF family had surprisingly little effect on hematopoiesis in steady state and functional HSC defects were only apparent after serial transplantations[5].

Normally, HIF-1α activity is regulated on a post-transcriptional, post-translational level by oxygen dependent hydroxylation of two proline residues in the oxygen-dependent domain (ODD) of the HIF-1α subunit followed by binding of the von Hippel Lindau (VHL) protein and degradation by the ubiquitination pathway[6]. Other mechanisms than oxygen tension might regulate HIF-1α expression in the HSC niche. Cytokines, like stem cell factor (SCF) and thrombopoetin (TPO) that are highly expressed in the adult bone marrow (BM) niche have been shown to lead to HIF-1α stabilization[7, 8]. Moreover, the homeobox gene Meis1, highly expressed in HSCs, also stabilizes HIF-1α contributing to the quiescence of HSCs[9].

Members of the HIF family have been proposed to be crucial for self-renewal of human acute myeloid leukemia-initiating cells (AML-ICs). shRNA expression against HIF-1/2α in human AMLs showed impaired engraftment in NOD/SCID mice[10, 11]. Whether HIF was a direct target of the genetic alterations in the used AML samples has not been

addressed in these studies. On the other hand, Meis1, commonly overexpressed in AML, induces HIF-1α stabilization, and accordingly, its deletion in transgenic mice leads to HSCs exhaustion due to their inability to up-regulate HIF-1α[9, 12].

Additionally, it has been shown that the t(9;21) fusion protein BCR-ABL signals directly to HIF-1α leading to its activation[13]. Deletion of HIF-1α in a murine model of chronic myeloid leukemia (CML) showed that CML-initiating cells (CML-ICs) lacking HIF-1α failed to generate leukemia in secondary transplanted mice arguing for an important role of HIF-1α in CML-ICs self-renewal[14].

Taking all these data into consideration, HIF-1α might be a good therapeutic target for different types of leukemia if HSCs and leukemic initiating cells (LICs) had a different requirement for HIF signaling. Since previous studies have used methods (shRNA expression, unspecific inhibitors of HIF in human AML cells or retroviral transduction/transplantation assays)[10, 11] that could bear potential technical problems in the evaluation of LICs self-renewal, we have tested the requirement of HIF-1α in myeloproliferative neoplasms (MPN) using a FLT-3$^{ITD}$ transgenic mouse model. Internal tandem duplications (ITD) in the *FLT*3 gene are found in approximately 25% of AML cases, constitutively activating this receptor and predicting increased relapse rates and reduced overall survival[15].

Here, we show that loss of HIF-1α leads to an enhanced FLT-3$^{ITD}$-induced MPN phenotype, indicated by higher numbers of white blood cells (WBC) and myeloid cells, more severe splenomegaly and a shorter survival. The increased proliferation is cell-intrinsic and this phenotype transplantable to primary recipient mice. Our data question the role of HIF-1α as a target to eliminate LICs in MPN and show that loss of HIF-1α can aggravate the disease.

## Materials and methods:

### Transgenic mice

*Hif-1α*$^{flox/flox}$ mice[16] were crossed with the interferon-inducible *Mx1-Cre* mice[17] and with the knock-in *Flt-3*$^{ITD}$ mice[18] to generate conditional knock-out *Hif-1α*$^{flox/flox}$; *Mx1-Cre; Flt-3*$^{ITD/+}$ mice. All animals were bred and maintained in accordance with Lund University's ethical regulations (Ethical permit M86-12).

### Monitoring of mice and bone marrow transplantation assays

Leukemia development was analyzed by measuring myeloid cells and total WBC in peripheral blood (PB) every 4 weeks. Myeloid cells were analyzed by flow cytometry and WBC counts were determined by a cell counter (KX-21N, Sysmex, Norderstedt Germany).

For HSC transplantation, 8 to 12-week-old B6SJL (CD45.1) recipient mice were lethally irradiated with 900 cGy 4-15 hours prior to transplantation. BM c-kit$^+$ cells from donors (CD45.2) were isolated using the MACS® magnetic separation system and anti-c-kit magnetic beads (Miltenyi Biotec, Bergisch Gladbach, Germany). 5 x $10^5$ c-kit$^+$ cells were injected into the tail vein of recipient mice accompanied by 2 x $10^5$ freshly isolated total BM supporting cells from B6SJL x C57BL/6J (CD45.1-CD45.2) mice. Donor chimerism and myeloproliferative development were determined after transplantation by PB analysis every 4 weeks.

For the transplantation of the cells kept *in vitro*, c-kit$^+$ cells were cultured in serum free expansion media (StemCell Technologies, Vancouver, BC, Canada) supplemented with 20 ng/mL murine interleukin 3 (PeproTech, Stockholm, Sweden), 50 ng/mL human

interleukin 6 (PeproTech), 50 ng/mL human TPO (PeproTech) and 50 ng/mL murine SCF (PeproTech) for 48 hours before transplant.

Animals that had to be euthanized due to non-MPN-associated symptoms were excluded from the survival analysis.

Deletion of *Hif-1α* was verified by polymerase chain reaction (PCR) analysis of DNA from BM cells of primary animals using the following primers: HIFΔ-*forward*: 5' – GCAGTTAAGAGCACTAGTTG-3' and HIFΔ-*reverse*: 5' –TTGGGGATGAAAACATCTGC-3'.

**Flow cytometry analysis**

Expansion of the MPN and engraftment of transplanted cells were monitored by flow cytometry analysis of PB, BM and spleen cells. PB samples were lysed with ammonium chloride (StemCell Technologies) prior to staining. 4,6 diamidino-2-phenylindole (DAPI) (Sigma-Aldrich, St. Louis, MO, USA) or 7-amino-actinomycin D (7-AAD, BD Pharmingen, San Diego, CA, USA) was used to exclude dead cells. For chimerism and lineage analysis the following antibodies were used: Gr1-PE, -PECy5 (RB6-8C5), Mac1-PE, -PECy5 (M1/70), B220-PE, -APC, -PECy5 (RA3-6B2), CD3-PE, -PECy5 (145-2C11), Ter119-PECy5 (TER-119), CD45.1-PECy7 (A20), Sca1-BV, -APC (D7), CD48-FITC (HM48-1) and CD150-APC, -PECy7 (TC15-12F12.2) from BioLegend (San Diego, CA, USA) and CD45.2-APCe780 (104) and c-kit-APCe780 (2B8) from eBiosciences (San Diego, CA, USA).

For cell cycle analysis, cells were fixed in 0.4% formaldehyde (Merck, Darmstadt, Germany) and permeabilized with 0.1% Triton-X (Sigma-Aldrich). Thereafter, cells were stained with Ki-67-PE (B56) antibody (BD Pharmingen) and DAPI (Sigma-Aldrich). Cellular reactive oxygen species (ROS) production was analyzed using

CellROX® Deep Red Reagent (Life Technologies, Stockholm, Sweden); mitochondrial ROS production was analyzed using MitoSOX™ Red mitochondrial superoxide indicator (Life Technologies) at 2 μM concentration; mitochondrial activity was evaluated using MitoTracker® Deep Red FM probe (Life Technologies) at 10 nM concentration; apoptosis analysis was performed using the BD Pharmingen™ PE Annexin Apoptosis Detection Kit (BD Pharmingen); all according to manufacturer's instructions. Samples were analyzed using a FACSCantoII (BD Biosciences, Stockholm, Sweden) and data was analyzed with FlowJo software (TreeStar, Ashland, OR, USA ).

**Histology**

For morphological analysis, cells from BM and spleen were subjected to cytospin preparation onto glass slides and PB smears were stained with May-Grünwald (Merck) and Giemsa (Merck). For microscopic examination, an Olympus IX70 microscope and an Olympus DP72 camera were used (Olympus, Tokyo, Japan).

**Statistical analysis**

All data are expressed as the mean ± SEM. Differences between groups were assessed by unpaired two-tailed Student's t-test. Statistical analysis of survival curves was performed using Mantel-Cox log-rank test. All analyses were performed with Prism software version 6.0 (GraphPad Software, San Diego, CA, USA). Animal cohort size was chosen according to the published literature and our previous studies. Since all experiments were performed with mice homogeneous regarding strain and age, no randomization method was used. Since this study did not include objective measurements, no blinding was performed.

**Results:**

**Spontaneous deletion of *Hif-1α* by *Mx1*-Cre in the FLT-3$^{ITD}$ mice**

To investigate the role of HIF-1α in FLT-3$^{ITD}$-induced MPN and self-renewal of LICs, *Flt-3*$^{ITD}$ knock-in mice were crossed with *Hif-1α* conditional knock-out mice and *Mx1*-Cre mice to obtain *Flt-3*$^{ITD/+}$; *Hif-1α*$^{flox/flox}$; *Mx1*-Cre mice and *Flt-3*$^{ITD/+}$; *Hif-1α*$^{flox/flox}$ control mice (refer hereafter as *Hif-1α*$^{\Delta/\Delta}$ and *Hif-1α*$^{+/+}$, respectively). The phenotype of the FLT-3$^{ITD}$-induced MPN mouse model resembles human chronic myelomonocytic leukemia (CMML), with an expansion of the myeloid/monocytic compartment[18]. We intended to delete the *Hif-1α* gene using poly(deoxyinosinic/deoxycytidylic) acid (pIpC) for induction of the Cre recombinase under the control of the *Mx1* promoter. However, investigation of untreated mice showed that recombination had occurred spontaneously, probably due to activation of signaling pathways downstream of the *Flt3* receptor, triggering an interferon response and leading to the expression of Cre recombinase (Figure 1a and Supplementary Figure S1). Due to the very high spontaneous deletion frequency of the floxed HIF-1α gene none of the mice were treated with pIpC.

**FLT-3$^{ITD}$-induced MPN is aggravated by the loss of HIF-1α**

Primary *Hif-1α*$^{\Delta/\Delta}$ mice surprisingly showed a more severe FLT-3$^{ITD}$ MPN phenotype than *Hif-1α*$^{+/+}$ animals. While control mice suffered from a chronic MPN that mice normally did not succumb to, *Hif-1α*$^{\Delta/\Delta}$ mice started to die at week 26 of age, reaching 50% of survival at week 68 (Figure 1b). This enhanced MPN phenotype was also reflected in higher WBC counts (Figure 1c) and a higher percentage of Gr1$^{+}$/Mac1$^{+}$

cells (myeloid cells) in PB at 8, 12, 16 and 20 weeks of age (Figure 1d-e and Supplementary Figure S2). Blood smears also showed more mature granulocytes in *Hif-1*$\alpha^{\Delta/\Delta}$ mice (Figure 1f).

20-week-old mice were sacrificed to analyze other MPN symptoms. Bones from mice lacking HIF-1α presented pale aspect (femurs, tibiae and hips) (Figure 2a), probably due to a combination of anemia (Table 1) and infiltration of myeloid cells in the BM. FLT-3$^{ITD}$-induced MPN in the absence of HIF-1α was characterized by a more severe splenomegaly and hepatomegaly indicated by higher spleen and liver weights (Figure 2a-b) in *Hif-1*$\alpha^{\Delta/\Delta}$ mice. Percentages of Gr1$^+$/Mac1$^+$ cells in BM and spleen were also increased upon loss of HIF-1α (Figure 2c-d). Taken together, our data indicate that loss of HIF-1α in an FLT-3$^{ITD}$-induced MPN model accelerates disease progression and aggravates its severity.

**Loss of HIF-1α affects cell cycle status of FLT-3$^{ITD}$-induced MPN cells**

To investigate whether higher number of myeloid cells in PB, BM and spleen was due to increased proliferation or decreased apoptosis, we first investigated cell cycle status in malignant myeloid cells from these tissues. Cell cycle analysis revealed that there was a higher percentage of cycling cells in spleen (G2/S/M phase) of *Hif-1*$\alpha^{\Delta/\Delta}$ mice compared to controls (Figure 2e and Supplementary Figure S3). Interestingly we observed no differences in BM cells from mice with different HIF-1α status. Overall these data indicate that loss of HIF-1α in FLT-3$^{ITD}$-induced MPN results in an increased number of Gr1$^+$/Mac1$^+$ myeloid cells by enhance proliferation in spleen as shown by a higher percentage of cycling cells, even when expressing maturation surface markers.

When studying cell death of these neoplastic myeloid cells, we observed that loss of HIF-1α leads to a decrease in apoptosis both in BM and spleen (Figure 2f-g).

Our data point to a dual role of HIF-1α loss in the observed phenotype by increasing the percentage of cells in active cycling and at the same time decreasing apoptosis resulting in an overall more severe MPN phenotype.

**Loss of HIF-1α leads to an organ-specific change in stem and progenitor cell numbers**

It has been previously shown that *Flt-3*$^{ITD/+}$ mice present an expansion of multi-potent progenitor cells (MPPs) and a severe decrease in long-term hematopoietic stem cells (LT-HSCs) using either CD48/CD150 (SLAM) or FLT-3/CD34 staining of Lin-, Sca-1$^{+}$, c-Kit$^{+}$ (LSK) cells[15, 19, 20]. Having shown that deletion of *Hif-1*α leads to an enhanced FLT-3$^{ITD}$-induced MPN we wanted to further characterize at which level of the hematopoietic hierarchy the effects occur. For this reason we analyzed and enumerated different hematopoietic stem and progenitor populations using staining for LSK and SLAM markers. Since expression of FLT-3$^{ITD}$ leads to an expansion of mature granulocytes in BM resulting in a change of cellular composition, both, percentages and total numbers of cells were analyzed (Figure 3a-c and Supplementary Figure S4). We observed the previously described reduction of LT-HSCs (LSK CD48$^{-}$ CD150$^{+}$) in FLT-3$^{ITD}$ expressing mice compared to wild type (wt) mice, but even to a bigger extent when *Hif-1*α was deleted. When comparing BM cells from *Hif-1*α$^{\Delta/\Delta}$ mice to controls, we found an expansion of the more mature compartment (LK cells: Lin- c-Kit+ Sca1-) and a progressive decrease towards LT-HCSs, through the different levels of differentiation (LSK and MPPs (defined as LSK CD48- CD150-)). In spleen, the

scenario was different, showing an increment (although non-significant in some cases) of cells of all these different undifferentiated populations in the *Hif-1*$\alpha^{\Delta/\Delta}$ mice.

When analyzing cell cycle status of these populations, we only observed higher percentage of cycling cells (G1-G2 phase) in *Hif-1*$\alpha^{\Delta/\Delta}$ mice in the LSK population in spleen (Figure 3d and Supplementary Figure S5). These results, together with data presented in Figure 2e, indicate that the production of malignant cells in the *Hif-1*$\alpha^{\Delta/\Delta}$ mice occurs mainly in the spleen through proliferation of committed progenitors.

Thus, the lost of HIF-1α changes the phenotype of FLT-3$^{ITD}$ malignancies in terms of proportions and location of primitive cells.

**The effect of HIF-1α loss on FLT-3$^{ITD}$-induced MPN is cell-intrinsic**

To investigate whether the aggravation of the FLT-3$^{ITD}$-induced MPN by HIF-1α loss is a cell intrinsic effect or a result mediated by cells in the microenvironment, and if this loss results in a defect in LICs homeostasis and self-renewal, transplantation assays were performed. To this end, c-kit$^{+}$ BM cells from the different genotypes were transplanted into lethally irradiated recipient wt mice.

The disease was transplantable and additionally, the acceleration of the MPN phenotype by loss of HIF-1α was also observed in transplanted mice with *Hif-1*$\alpha^{\Delta/\Delta}$ cells, arguing for a cell-intrinsic effect of HIF-1α on FLT-3$^{ITD}$-induced MPN (Figure 4a and Supplementary Figure S6). However, the reduction in LT-HSCs observed in transgenic animals (Supplementary Figure S6f) is more severe in transplanted mice and accordingly, secondary recipients showed a loss of *Hif-1*$\alpha^{\Delta/\Delta}$ donor contribution to PB (Supplementary Figure S7). The fact that *Hif-1*$\alpha^{\Delta/\Delta}$ FLT-3$^{ITD}$ MPN was transplantable into primary recipients indicates that loss of HIF-1α did not result in a defect in LICs

267 engraftment, although the numbers of LT-HSCs are severely affected in primary
268 recipients. Whether the effect in the secondary recipients is due to a loss of LIC self-
269 renewal or a displacement of LT-HSC by expanding MPPs in the bone marrow remains
270 elusive.

271 Previous studies, investigating the role of HIF-1α in CML, have used a retroviral
272 transduction/transplantation model that requires cycling of the hematopoietic stem
273 and progenitor cells (HSPCs), which is normally induced by *in vitro* culturing in the
274 presence of cytokines. To test whether these experimental differences could explain
275 the conflicting results between our experiments and previously published data, we
276 cultured c-kit$^+$ BM cells in presence of cytokines, as normally performed when using
277 the transduction/transplantation method, and transplanted afterwards. Mice
278 transplanted with *in vitro* cultured *Hif-1*$\alpha^{\Delta/\Delta}$ BM cells showed, not only, a similar
279 phenotype regarding the expansion of myeloid cells over time, but also a shorter
280 survival ($P$=0.0046)(Figure 4b and Supplementary Figure S8a-b). Mice transplanted
281 with *Hif-1*$\alpha^{\Delta/\Delta}$ cultured BM cells started to die of progressive MPN around week 20
282 with most of the animals dead by week 40, while no animal died in the control group.

283 To evaluate the level of competition in our transplantation experiments, we calculated
284 the number of LT-HSCs injected in each group. According to the obtained values in
285 Figure 3 of c-kit$^+$ cells and LT-HSCs in wt, *Hif-1*$\alpha^{+/+}$ and *Hif-1*$\alpha^{\Delta/\Delta}$ animals, we estimated
286 that the ratio of competitor:donor cells was 1:3 for *Hif-1*$\alpha^{\Delta/\Delta}$ and 1:65 for *Hif-1*$\alpha^{+/+}$ cells
287 respectively. Beside the higher competition in the *Hif-1*$\alpha^{\Delta/\Delta}$ group, we observed similar
288 levels of donor contribution to the myeloid compartment 20 weeks post-
289 transplantation (Supplementary Figure S8c). To analyze donor contribution to the
290 other cell lineages discarding the effect of the percentage variation when one

population is highly increased, we calculated donor contribution to each lineage in total number of cells. We observed equal contribution to the T cells from *Hif-1*$\alpha^{+/+}$ and *Hif-1*$\alpha^{\Delta/\Delta}$ animals. However, we observed more contribution from *Hif-1*$\alpha^{\Delta/\Delta}$ donor cells to myeloid and less to B cell lineage most likely due to the MPN phenotype resulting in an expansion of myeloid cells at the expense of B-cells (Supplementary Figure S8d).

In summary, our data indicate that FLT-3$^{ITD}$-induced MPN is cell-intrinsic and transplantable, independently of HIF-1α status. Self-renewal of LICs was not lost even when cells were cultured *in vitro* for 48 hours prior to primary transplantations, although LT-HSCs numbers are highly reduced in recipient mice transplanted with *Hif-1*$\alpha^{\Delta/\Delta}$.

**HIF-1α status influences mitochondrial activity and ROS levels in FLT-3$^{ITD}$-induced MPN**

Mitochondrial respiratory chain constitutes the main intracellular source of ROS in most of the tissues. Because HIF-1α status influences the metabolism of cells[3], which could affect the malignant properties of the FLT-3$^{ITD}$ cells, we examined mitochondrial membrane function and levels of ROS of these neoplastic myeloid cells. Two different tests showed an increment of cellular and mitochondrial ROS levels in *Hif-1*$\alpha^{\Delta/\Delta}$ mice in BM and an opposite effect in spleen (Figure 5a-b).

According to mitochondrial membrane function, we found three well-defined different populations, named as M1, M2 and M3 (Figure 5c). Whereas in BM there was an increase in the population with less mitochondrial activity (M1) when *Hif-1*α is deleted, we observed a reduction of this population in the splenic myeloid cells. This

could be indicating that high ROS production is a result of higher mitochondrial function caused by higher metabolic activity of *Hif-1*$\alpha^{\Delta/\Delta}$ cells.

Together this data could indicate a metabolic adaptation of these malignant cells to their new niches and an improvement of their tumorigenic capacities (less quiescence and more proliferation) when HIF-1α is lost in these cells.

**Discussion:**

Hypoxia signaling, mainly mediated by transcription factors HIF-1α and HIF-2α and their target genes, has been shown to play an important role in stem cell biology, particularly in normal and malignant HSPCs. Previous work has provided evidence that HIF-1α is required for HSCs quiescence and self-renewal[2] as well as HIF-2α has a role in protecting HSCs from endoplasmic reticulum stress-induced apoptosis[11]. Surprisingly, loss of HIF-1α function (and combined loss of HIF-1α and HIF-2α) seems rather weak since the phenotype comes only apparent after challenging HSCs by serial transplantation[2, 5].

Additionally, it has been demonstrated that HIF might play a role in murine and human leukemia. Inhibitors and shRNA against HIF-1α and HIF-2α have been used to show the requirement of these two transcription factors in human AML-ICs self-renewal and ability to induce AML in immune-compromised mice[10, 11].

The concept to target HIF in AML is intriguing but whether there is a therapeutic window for the treatment of leukemia by targeting HIF-1/2α without inducing major hematologic toxicity has not been extensively studied. It also remains elusive whether HIF can function as a therapeutic target for all genetic subtypes of AML. It has been shown that some genetic alterations in AML stabilize HIF in a hypoxia-independent

manner, making these specific subtypes maybe prime targets for therapy against HIF. Requirement of HIF-1α for CML-ICs self-renewal has been confirmed using retroviral overexpression of BCR-ABL oncogene in BM cells from HIF-1α conditional knock-out mice[14]. All these approaches have some technical caveats that could influence the viability of LICs. First, inhibitors of HIF-1α are rather unselective making it difficult to evaluate whether their effect is primarily caused by HIF-1α inhibition. Expression of shRNA against HIF family members requires retroviral transduction of AML-LICs and might have off-target effects even though scrambled shRNA was used as control. Retroviral transduction of BM cells requires cytokine stimulation of HSPCs *in vitro,* which can change the properties of these cells. Therefore, we have investigated the role of HIF-1α in FLT-3$^{ITD}$-induced MPN using just transgenic mouse models for both genetic alterations.

The first unexpected result was a spontaneous deletion of the floxed *Hif-1α* gene in *Flt-3*$^{ITD}$; *Mx1*-Cre background. We assume that FLT-3$^{ITD}$ signaling triggers an interferon response that leads to activation of Cre recombinase via activation of *Mx1* promoter. Our finding is in accordance with the published literature[20, 21] in which mice with either *Runx1*$^{flox/flox}$ or *Npm1*$^{flox\text{-}cA/+}$ in combination with a *Flt-3*$^{ITD}$ and *Mx1*-Cre genotype develop AML spontaneously.

In contrary to the previously described role of HIFs in LICs of AML and CML, we found that HIF-1α lost exaggerates FLT-3$^{ITD}$-induced MPN phenotype, as indicated by a shorter survival, higher number of myeloid cells in PB, BM and spleen, leading to a more severe splenomegaly.

It has been previously shown that *Flt-3*$^{ITD}$ knock-in mice have an expansion of the myeloid progenitor compartment while the LT-HSC population was severely

decreased[15, 19, 20]. We observed that this effect is even more aggravated when *Hif-1α* is deleted. Surprisingly, reduction of LT-HSCs was not associated with a dramatic loss of LICs homeostasis, since the MPN could be transplanted into primary recipient animals even after *in vitro* incubation. Interestingly, transplanted MPNs lacking HIF-1α showed an even more aggressive phenotype as indicated by a shorter survival of transplanted mice. Whether the reduction in LT-HSCs in the bone marrow of primary recipients and the associated low contribution of *Hif-1α*$^{\Delta/\Delta}$ cells in the secondary recipients is due to a defect in self-renewal or a displacement by progenitors and mature myeloid cells needs further investigation.

Hypoxia-induced HIF expression has been linked to metabolic switch due to a shift from oxidative phosphorylation (OXPHOS) to glycolysis, an effect that has been first described by Warburg and carries his name[22]. Tumors that become hypoxic heavily depend on this mechanism but even tumors that are not hypoxic switch to energetically very inefficient glycolysis for reasons that still remain elusive. Therefore, we investigated the metabolic profile (mitochondrial function and ROS levels) of FLT-3$^{ITD}$-MPN cells lacking HIF-1α. It has been described that changes in these parameters can affect self-renewal and differentiation of HSCs. For instance, when mitochondrial potential is blocked, HSCs are unable to initiate differentiation[23] and high levels of ROS force cells to go out of quiescence[24, 25]. We found a correlation between cycling profile, ROS levels an mitochondrial function in FLT-3$^{ITD}$-MPN cells (Figure 5d), indicating a more active status of *Hif-1α*$^{\Delta/\Delta}$ cells in spleen, the main (malignant) hematopoietic organ in animals with MPN and leading to a more aggressive disease.

The fact that, in animals with the MPN, hematopoiesis is taking place in an extramedullary niche (spleen), with very different microenvironmental properties

from the BM, including oxygen tension, lead us to postulate that these observed differences are established by cell-intrinsic mechanisms that stabilize HIF-1α, imprinted already in the primary niche (BM) or by originating genetic alterations of the malignancy.

These results are in concordance with our recently findings regarding the role of HIF-1α in AML pathogenesis using oncogenes that either do or do not signal directly towards HIF-1α. Expression of *MLL-AF*9 and *MEIS1/HOXA9,* that are supposedly activating HIF-1α, and *AML/ETO9a*, a truncated version of the AML1/ETO fusion protein with no known connection to HIF-1α, induced AML independent of HIF-1α status[26]. HIF-1α was not needed for LIC self-renewal, but loss of HIF-1α rather lead to an accelerated and more severe phenotype, similar to the observations made for the FLT-3$^{ITD}$ -induced MPN model described in this paper.

Based on previous studies, it has been proposed that HIF might be used as molecular therapeutic target to interfere with self-renewal of LICs. Our data indicate that targeting HIF-1α in FLT-3$^{ITD}$-induced MPN rather leads to disease acceleration and a more severe phenotype. Whether the inhibition of HIF in combination with chemotherapy or targeted small molecules can be a useful therapeutic strategy needs further investigation.

**Conflict of Interest**

The authors declare no conflict of interest.

**Acknowledgements**

The authors thank Dr. D. Gary Gilliland (University of Pennsylvania, Philadelphia, USA) for kindly providing *Flt-3*$^{ITD}$ knock-in mice and Dr. David Bryder (Lund University, Lund, Sweden) for helpful discussions and advice on flow cytometry.

This work was supported by project grants from Barncancerfonden, Cancerfonden and SSF through the Hemato-Linné and StemTherapy consortium (Sweden) to J.C. and a post-doctoral grant from Barncancerfonden (Sweden) to T.V.-H.

**Author's contributions**

T.V.-H. designed the research, performed experiments, analyzed data, created figures, and wrote the manuscript; D.T. performed experiments; J.C. conceived and supervised the project, designed the research, and wrote the manuscript. All authors read and approved the final manuscript.

## References

1. Nilsson SK, Johnston HM, Coverdale JA. Spatial localization of transplanted hemopoietic stem cells: inferences for the localization of stem cell niches. *Blood* 2001 Apr 15; **97**(8)**:** 2293-2299.

2. Takubo K, Goda N, Yamada W, Iriuchishima H, Ikeda E, Kubota Y*, et al.* Regulation of the HIF-1alpha level is essential for hematopoietic stem cells. *Cell stem cell* 2010 Sep 3; **7**(3)**:** 391-402.

3. Takubo K, Nagamatsu G, Kobayashi CI, Nakamura-Ishizu A, Kobayashi H, Ikeda E*, et al.* Regulation of glycolysis by Pdk functions as a metabolic checkpoint for cell cycle quiescence in hematopoietic stem cells. *Cell stem cell* 2013 Jan 3; **12**(1)**:** 49-61.

4. Rehn M, Olsson A, Reckzeh K, Diffner E, Carmeliet P, Landberg G*, et al.* Hypoxic induction of vascular endothelial growth factor regulates murine hematopoietic stem cell function in the low-oxygenic niche. *Blood* 2011 Aug 11; **118**(6)**:** 1534-1543.

5. Guitart AV, Subramani C, Armesilla-Diaz A, Smith G, Sepulveda C, Gezer D*, et al.* Hif-2alpha is not essential for cell-autonomous hematopoietic stem cell maintenance. *Blood* 2013 Sep 5; **122**(10)**:** 1741-1745.

6. Semenza GL. Hypoxia-inducible factors in physiology and medicine. *Cell* 2012 Feb 3; **148**(3)**:** 399-408.

7. Pedersen M, Lofstedt T, Sun J, Holmquist-Mengelbier L, Pahlman S, Ronnstrand L. Stem cell factor induces HIF-1alpha at normoxia in hematopoietic cells. *Biochemical and biophysical research communications* 2008 Dec 5; **377**(1)**:** 98-103.

8. Kirito K, Fox N, Komatsu N, Kaushansky K. Thrombopoietin enhances expression of vascular endothelial growth factor (VEGF) in primitive hematopoietic cells through induction of HIF-1alpha. *Blood* 2005 Jun 1; **105**(11)**:** 4258-4263.

9. Simsek T, Kocabas F, Zheng J, Deberardinis RJ, Mahmoud AI, Olson EN*, et al.* The distinct metabolic profile of hematopoietic stem cells reflects their location in a hypoxic niche. *Cell stem cell* 2010 Sep 3; **7**(3)**:** 380-390.

10. Wang Y, Liu Y, Malek SN, Zheng P, Yang L. Targeting HIF1alpha eliminates cancer stem cells in hematological malignancies. *Cell stem cell* 2011 Apr 8; **8**(4)**:** 399-411.

11. Rouault-Pierre K, Lopez-Onieva L, Foster K, Anjos-Afonso F, Lamrissi-Garcia I, Serrano-Sanchez M*, et al.* HIF-2alpha protects human hematopoietic stem/progenitors and acute myeloid leukemic cells from apoptosis induced by endoplasmic reticulum stress. *Cell stem cell* 2013 Nov 7; **13**(5)**:** 549-563.

12. Hisa T, Spence SE, Rachel RA, Fujita M, Nakamura T, Ward JM*, et al.* Hematopoietic, angiogenic and eye defects in Meis1 mutant animals. *The EMBO journal* 2004 Jan 28; **23**(2)**:** 450-459.

13. Mayerhofer M, Valent P, Sperr WR, Griffin JD, Sillaber C. BCR/ABL induces expression of vascular endothelial growth factor and its transcriptional activator, hypoxia inducible factor-1alpha, through a pathway involving phosphoinositide 3-kinase and the mammalian target of rapamycin. *Blood* 2002 Nov 15; **100**(10)**:** 3767-3775.

14. Zhang H, Li H, Xi HS, Li S. HIF1alpha is required for survival maintenance of chronic myeloid leukemia stem cells. *Blood* 2012 Mar 15; **119**(11)**:** 2595-2607.

15. Chu SH, Heiser D, Li L, Kaplan I, Collector M, Huso D*, et al.* FLT3-ITD knockin impairs hematopoietic stem cell quiescence/homeostasis, leading to myeloproliferative neoplasm. *Cell stem cell* 2012 Sep 7; **11**(3)**:** 346-358.

16. Ryan HE, Poloni M, McNulty W, Elson D, Gassmann M, Arbeit JM*, et al.* Hypoxia-inducible factor-1alpha is a positive factor in solid tumor growth. *Cancer research* 2000 Aug 1; **60**(15)**:** 4010-4015.

17. Kuhn R, Schwenk F, Aguet M, Rajewsky K. Inducible gene targeting in mice. *Science* 1995 Sep 8; **269**(5229)**:** 1427-1429.

18. Lee BH, Tothova Z, Levine RL, Anderson K, Buza-Vidas N, Cullen DE*, et al.* FLT3 mutations confer enhanced proliferation and survival properties to multipotent progenitors in a murine model of chronic myelomonocytic leukemia. *Cancer cell* 2007 Oct; **12**(4)**:** 367-380.

19. Li L, Piloto O, Nguyen HB, Greenberg K, Takamiya K, Racke F*, et al.* Knock-in of an internal tandem duplication mutation into murine FLT3 confers myeloproliferative disease in a mouse model. *Blood* 2008 Apr 1; **111**(7)**:** 3849-3858.

20. Mead AJ, Kharazi S, Atkinson D, Macaulay I, Pecquet C, Loughran S*, et al.* FLT3-ITDs instruct a myeloid differentiation and transformation bias in lymphomyeloid multipotent progenitors. *Cell reports* 2013 Jun 27; **3**(6)**:** 1766-1776.

21. Mupo A, Celani L, Dovey O, Cooper JL, Grove C, Rad R*, et al.* A powerful molecular synergy between mutant Nucleophosmin and Flt3-ITD drives acute myeloid leukemia in mice. *Leukemia* 2013 Sep; **27**(9)**:** 1917-1920.

22. Denko NC. Hypoxia, HIF1 and glucose metabolism in the solid tumour. *Nature reviews Cancer* 2008 Sep; **8**(9)**:** 705-713.

23. Yu WM, Liu X, Shen J, Jovanovic O, Pohl EE, Gerson SL*, et al.* Metabolic regulation by the mitochondrial phosphatase PTPMT1 is required for hematopoietic stem cell differentiation. *Cell stem cell* 2013 Jan 3; **12**(1)**:** 62-74.

24. Tothova Z, Gilliland DG. FoxO transcription factors and stem cell homeostasis: insights from the hematopoietic system. *Cell stem cell* 2007 Aug 16; **1**(2)**:** 140-152.

25. Ito K, Suda T. Metabolic requirements for the maintenance of self-renewing stem cells. *Nature reviews Molecular cell biology* 2014 Apr; **15**(4)**:** 243-256.

26. Velasco-Hernandez T, Hyrenius-Wittsten A, Rehn M, Bryder D, Cammenga J. HIF-1alpha can act as a tumor suppressor gene in murine acute myeloid leukemia. *Blood* 2014 Dec 4; **124**(24)**:** 3597-3607.

559 **Figure legends**

560

561 **Figure 1. Loss of HIF-1α accelerates FLT-3$^{ITD}$-induced MPN phenotype.**

562

563 (**a**) Deletion of *Hif-1*α was checked by PCR amplification of DNA extracted from BM
564 cells of the analyzed mice. Shown is a representative gel indicating deletion of *Hif-1*α in
565 non-treated *Hif-1*α$^{flox/flox}$; *Mx1-Cre; Flt-3*$^{ITD/+}$ mice. (**b**) Kaplan-Meier survival curve of
566 FLT-3$^{ITD}$ mice (*Hif-1*α$^{\Delta/\Delta}$, n= 10; *Hif-1*α$^{+/+}$, n= 14). Log-rank (Mantel-Cox) test was used
567 to assess statistical significance. (**c**, **d**) Blood analysis of mice at different ages, showing
568 increased WBC (**c**) and myeloid cells (Gr1$^+$/Mac1$^+$ cells) (**d**) in *Hif-1*α$^{\Delta/\Delta}$ mice (*Hif-*
569 *1*α$^{+/+}$, n=23; *Hif-1*α$^{\Delta/\Delta}$, n=18; wt, n=6). (**e**) Representative FACS plots of PB cells of 12-
570 week-old mice, showing an increased myeloid population in PB of *Hif-1*α$^{\Delta/\Delta}$ mice.
571 Differentiated populations are stained with the following antibodies: CD3 for T cells
572 (T), B220 for B cells (B) and Gr1/Mac1 for myeloid cells (M). (**f**) Representative blood
573 smears of 12-week-old mice of both genotypes. Scale bar= 10μm.
574 Plots represent mean ± SEM. Unless otherwise stated, 2-tailed Student *t* test was used
575 to assess statistical significance. **P*<0.05, ***P*<0.01, ****P*<0.001. wt = wild type.

576

577 **Figure 2. Accumulation of *Hif-1*α$^{\Delta/\Delta}$-mature myeloid cells in spleen is due to**
578 **increased cycling and reduced cell death.**

579

580 (**a**) Representative phenotype of bones and spleens from 20-week-old mice with the
581 indicated genotypes. (**b**) Increment in spleen and liver weight in *Hif-1*α$^{\Delta/\Delta}$ 20-week-
582 old-mice as a consequence of accelerated MPN in these mice (n=12; wt, n=6). (**c**)

Percentage of mature myeloid cells ($Gr1^+/Mac1^+$) in BM and spleen of 20-week-old mice (n=12; wt, n=6). (**d**) Cytospins of BM cells with different genotypes showing the mature myeloid aspect of predominant cells in this compartment. Scale bar= 10μm. (**e**) Cell-cycle analysis of myeloid cells ($Gr1^+/Mac1^+$) from 3 independent experiments (16 to 20-week-old mice) (n= 12; wt, n=6). (**f**) Apoptosis analysis of myeloid cells ($Gr1^+/Mac1^+$) from 2 independent experiments (20-week-old mice) (wt, n=6; *Hif-1*$\alpha^{+/+}$, n=7; *Hif-1*$\alpha^{\Delta/\Delta}$, n=8). Plots represent mean ± SEM. Two-tailed Student *t* test was used to assess statistical significance. **P*<0.05, ***P*<0.01, ****P*<0.001

**Figure 3. LT-HSCs are highly reduced in BM and expanded in spleen of *Hif-1*$\alpha^{\Delta/\Delta}$ mice with FLT-3$^{ITD}$-induced MPN.**

(**a**) Percentage of the indicated populations of undifferentiated cells from total BM or spleen cells (wt, n=5; *Hif-1*$\alpha^{+/+}$, n=12; *Hif-1*$\alpha^{\Delta/\Delta}$, n=13). (**b**) Absolute number of cells from the indicated population of undifferentiated cells in the BM (6 bones: 2 femurs, 2 tibiae and 2 hips) or spleen (wt, n=5; *Hif-1*$\alpha^{+/+}$, n=8; *Hif-1*$\alpha^{\Delta/\Delta}$, n=7). (**c**) Representative FACS plots of BM samples from both genotypes showing the gating strategy used for the analysis of LT-HSCs, MPPs, LSK and LK cells. First shown plots derived from a previous gating of singlets, alive, lineage negative cells. (**d**) Cell-cycle analysis of the indicated populations of undifferentiated cells from BM or spleen (20-week-old mice) (n= 3; wt, n=6). Plots represent mean ± SEM. Two-tailed Student *t* test was used to assess statistical significance. **P*<0.05, ***P*<0.01, ****P*<0.001

**Figure 4. *Hif-1*α-deleted-FLT-3$^{ITD}$ MPN-initiating cells are able to engraft and recapitulate the disease in recipient mice.**

(**a**) BM cells from a single donor were transplanted, without previous culturing *in vitro*, into 2-3 lethally irradiated wt mice. We show the phenotype of transplanted disease by several parameters: Kaplan-Meier survival curve, WBCs and myeloid (Gr1$^+$/Mac1$^+$) cells in PB at the indicated time points after transplantation (*Hif-1*α$^{+/+}$, n=9; *Hif-1*α$^{\Delta/\Delta}$, n=7). (**b**) BM cells from 3 different donors of each genotype were pooled together, kept in culture for 2 days and transplanted into 7 lethally irradiated wt mice. We show the phenotype of transplanted disease by several parameters: Kaplan-Meier survival curve, WBCs and myeloid (Gr1$^+$/Mac1$^+$) cells in PB at the indicated time points after transplantation (n=7). Log-rank (Mantel-Cox) test was used to assess statistical significance of the survival curve. Plots represent mean ± SEM. Unless otherwise stated, 2-tailed Student *t* test was used to assess statistical significance. **P*<0.05, ***P*<0.01, ****P*<0.001

**Figure 5. Malignant infiltrating cells in spleen present higher metabolic profile and oxidative stress.**

We analyzed cellular levels of ROS (**a**), measured by CellROX Deep Red staining (n=16), and mitochondrial levels of ROS (**b**) measured by MitoSOX staining (*Hif-1*α$^{+/+}$, n=7; *Hif-1*α$^{\Delta/\Delta}$, n=8) in myeloid cells (Gr1$^+$/Mac1$^+$) of BM and spleen. Plots represent normalized MFI respect to controls (mean MFI set at 100%) of each experiment (2-4

631 independent experiments; 20-week-old mice). (**c**) Mitochondrial membrane function,
632 measured by MitoTracker Deep Red staining (*Hif-1*$\alpha^{+/+}$, n=8; *Hif-1*$\alpha^{\Delta/\Delta}$, n=9), in
633 myeloid cells ($Gr1^+/Mac1^+$) of BM and spleen. We observed 3 different populations
634 according to MitoTracker staining that we named M1, M2 and M3 from lower to higher
635 intensity. We determined the percentage of myeloid cells in each of these populations
636 (3 independent experiments; 20-week-old mice). (**d**) Summary of the metabolic profile
637 of *Hif-1*$\alpha^{\Delta/\Delta}$ and *Hif-1*$\alpha^{+/+}$ myeloid cells in the BM and spleen. Dashed lines indicate
638 statistically non significant data. Plots represent mean ± SEM. Two-tailed Student *t* test
639 was used to assess statistical significance. **P*<0.05, ***P*<0.01, ****P*<0.001
640
641

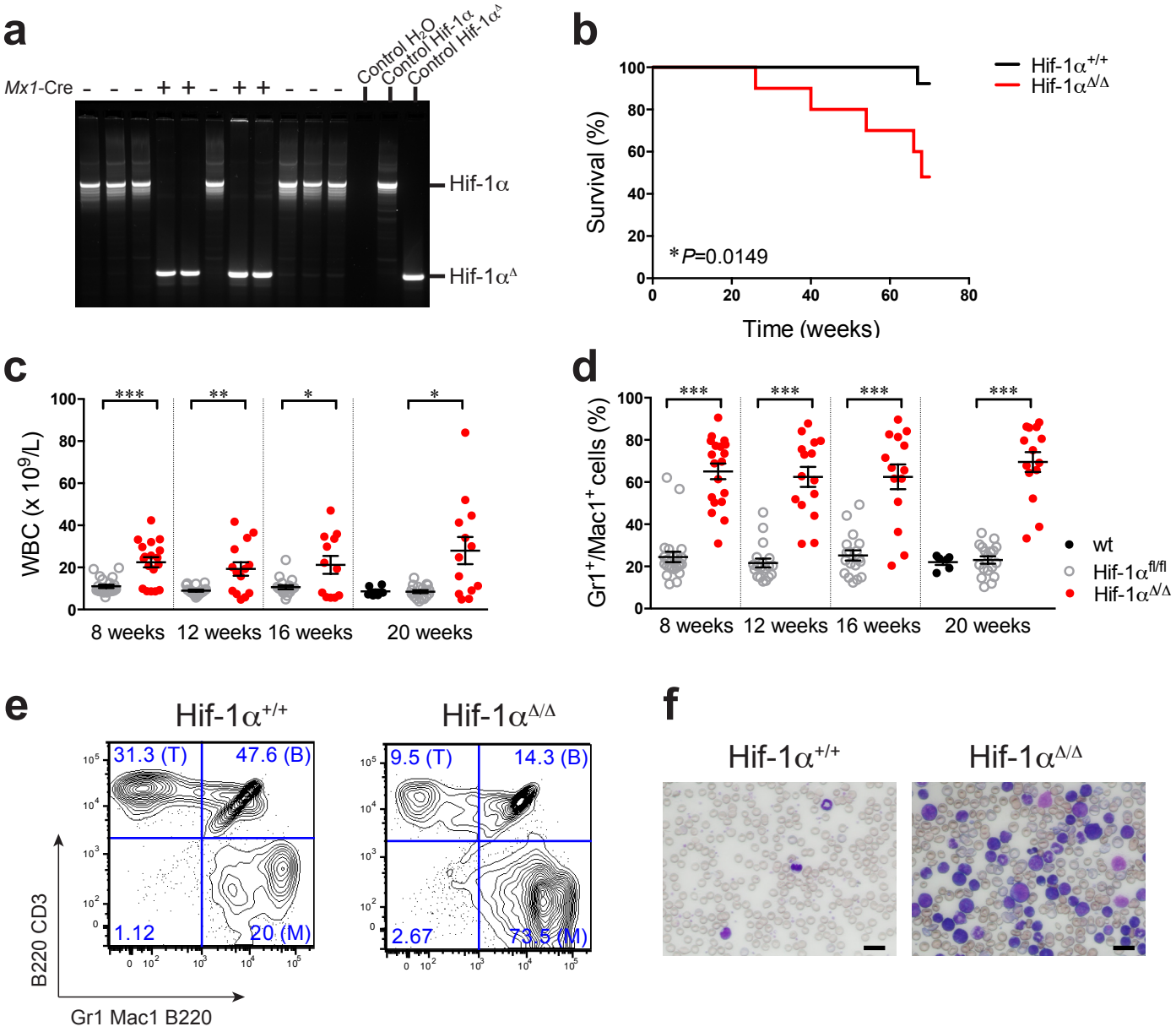
a
Mx1-Cre
Control H2O
Control Hif-1α
Control Hif-1αΔ
Hif-1α
Hif-1αΔ
b
Survival (%)
Time (weeks)
*P=0.0149
Hif-1α+/+
Hif-1αΔ/Δ
c
WBC (x 10^9/L)
8 weeks
12 weeks
16 weeks
20 weeks
d
Gr1+/Mac1+ cells (%)
wt
Hif-1αfl/fl
Hif-1αΔ/Δ
e
Hif-1α+/+
Hif-1αΔ/Δ
31.3 (T)
47.6 (B)
1.12
20 (M)
9.5 (T)
14.3 (B)
2.67
73.5 (M)
B220 CD3
Gr1 Mac1 B220
f
Hif-1α+/+
Hif-1αΔ/Δ

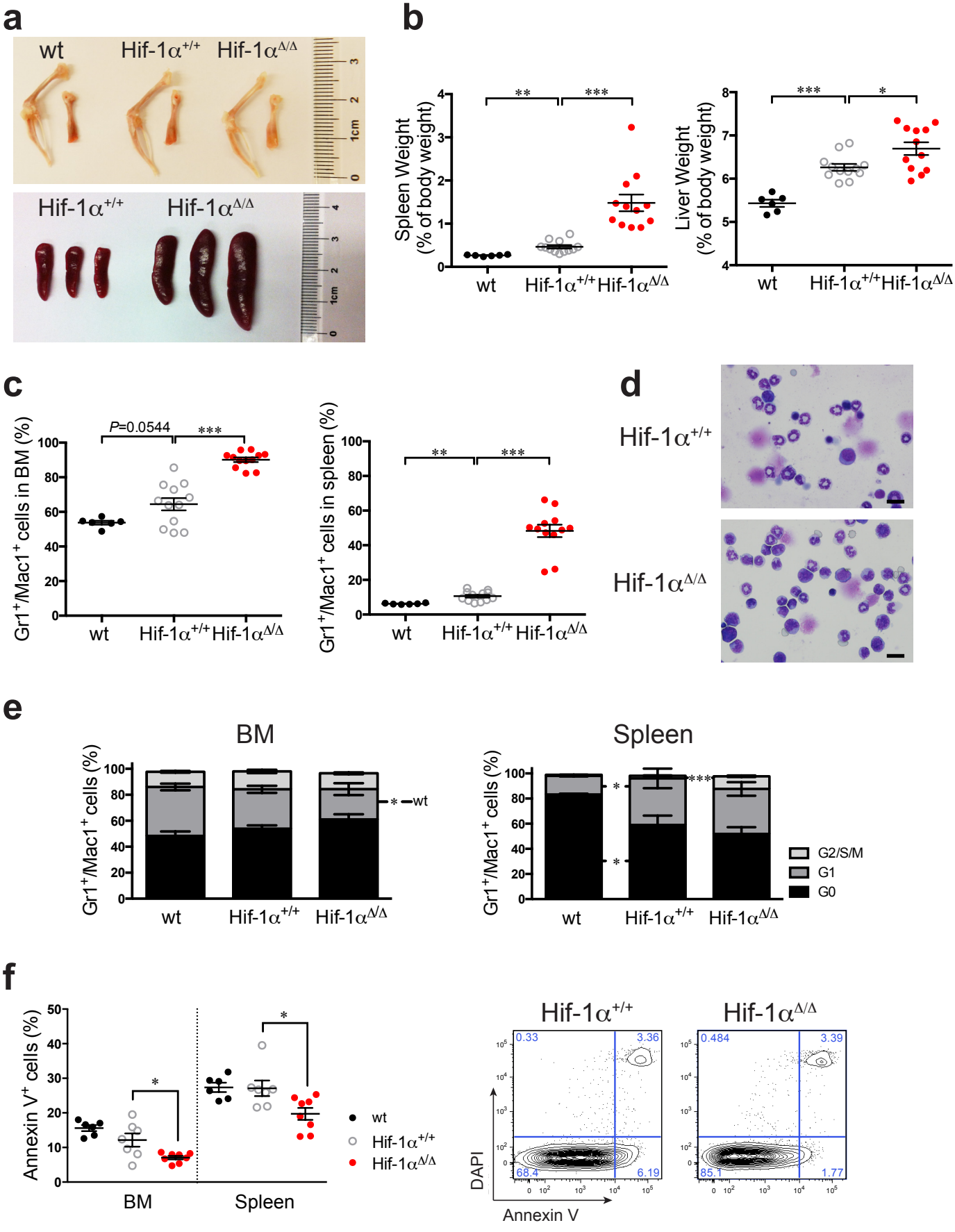
a
wt
Hif-1α+/+
Hif-1αΔ/Δ
b
Spleen Weight (% of body weight)
Liver Weight (% of body weight)
c
Gr1+/Mac1+ cells in BM (%)
P=0.0544
Gr1+/Mac1+ cells in spleen (%)
d
e
BM
Spleen
Gr1+/Mac1+ cells (%)
G2/S/M
G1
G0
f
Annexin V+ cells (%)
DAPI
Annexin V
0.33
3.36
68.4
6.19
0.484
3.39
85.1
1.77

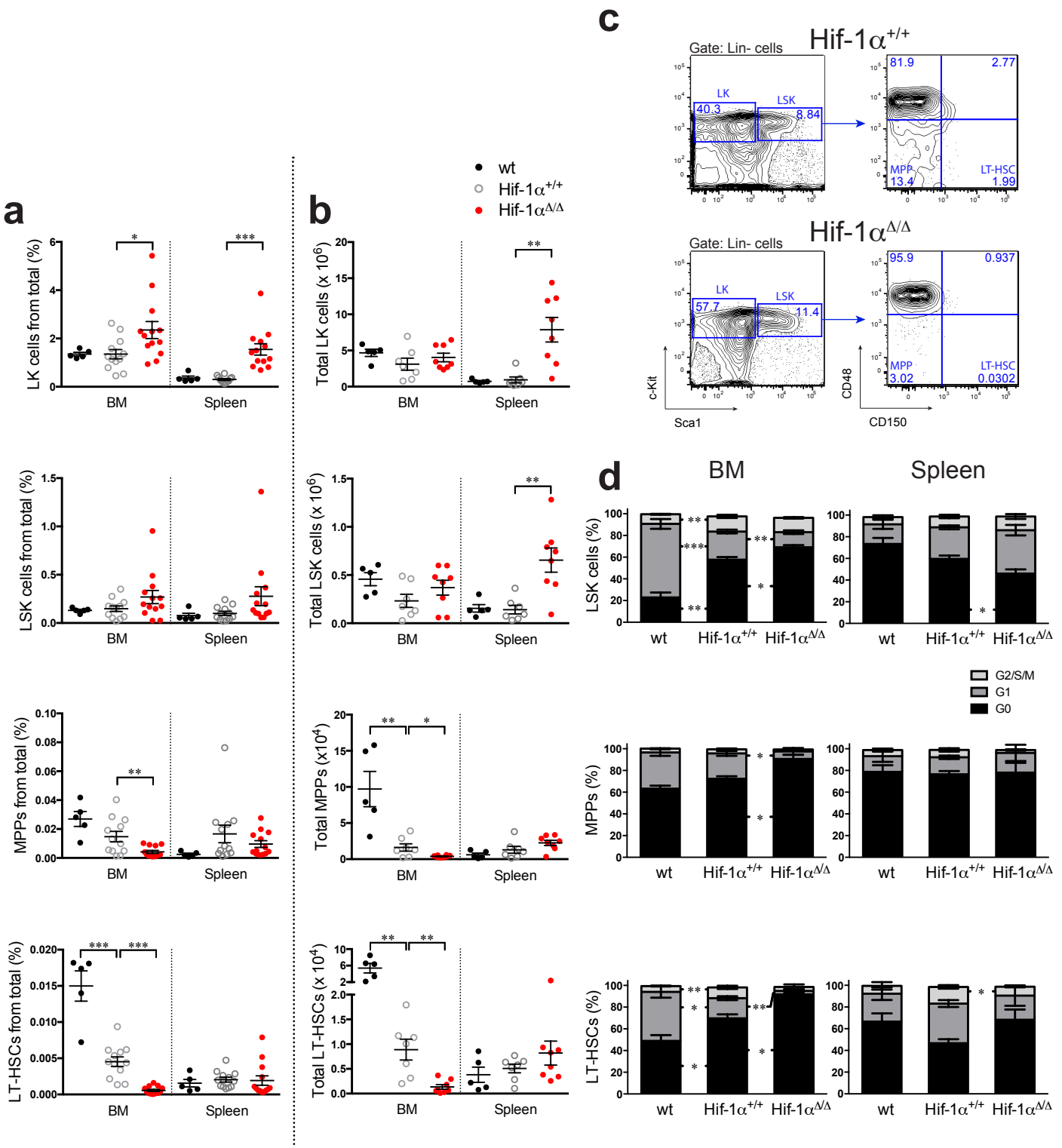
a
b
c
d
wt
Hif-1α+/+
Hif-1αΔ/Δ
LK cells from total (%)
Total LK cells (x 10^6)
LSK cells from total (%)
Total LSK cells (x 10^6)
MPPs from total (%)
Total MPPs (x10^4)
LT-HSCs from total (%)
Total LT-HSCs (x 10^4)
BM
Spleen
Gate: Lin- cells
LK
LSK
MPP
LT-HSC
40.3
8.84
13.4
1.99
81.9
2.77
57.7
11.4
3.02
0.0302
95.9
0.937
c-Kit
Sca1
CD48
CD150
LSK cells (%)
MPPs (%)
LT-HSCs (%)
G2/S/M
G1
G0

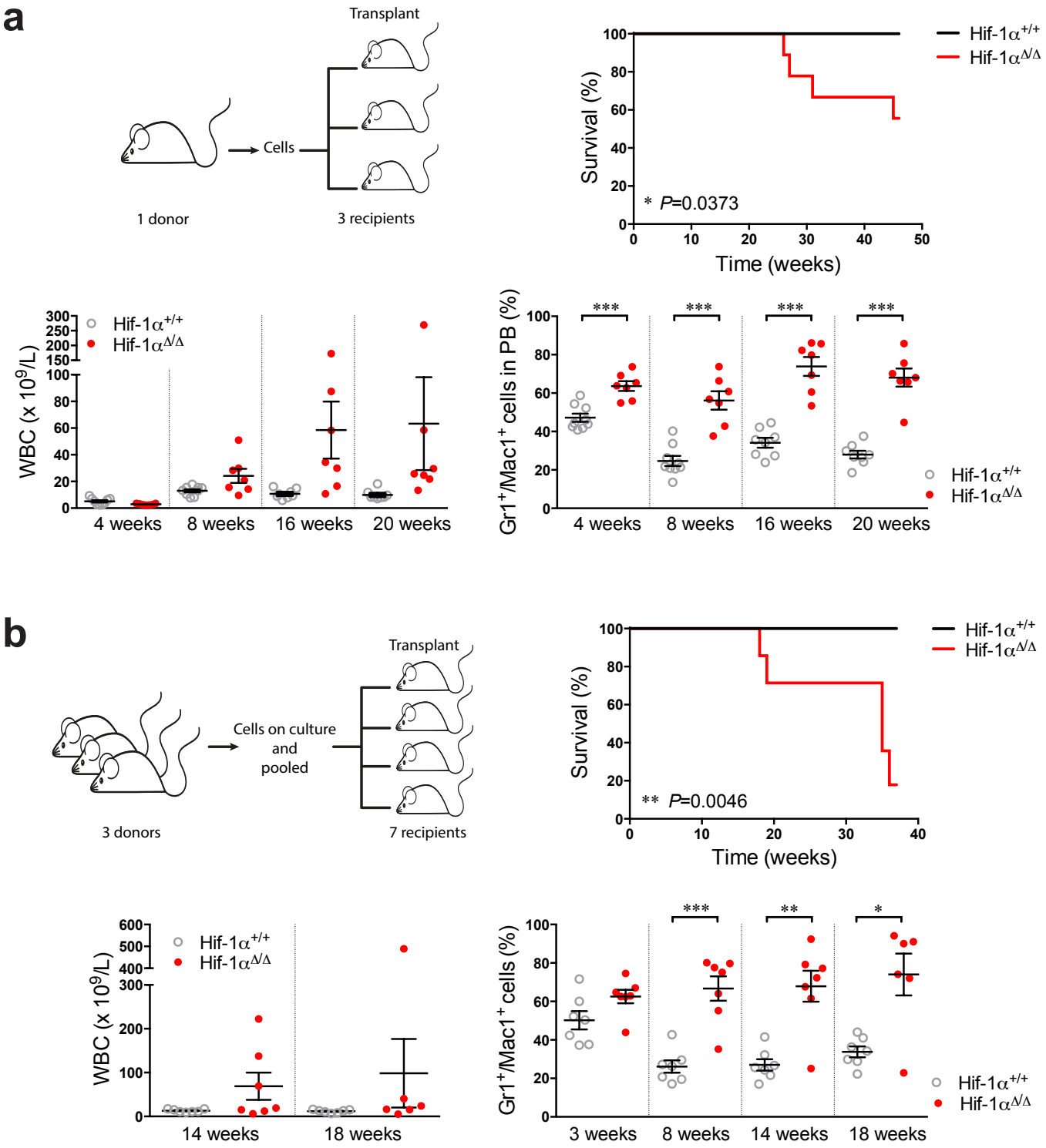
a
Transplant
Cells
1 donor
3 recipients
Survival (%)
Time (weeks)
* P=0.0373
Hif-1α+/+
Hif-1αΔ/Δ
WBC (x 10^9/L)
4 weeks
8 weeks
16 weeks
20 weeks
Gr1+/Mac1+ cells in PB (%)
***
b
Transplant
Cells on culture and pooled
3 donors
7 recipients
** P=0.0046
Gr1+/Mac1+ cells (%)
3 weeks
14 weeks
18 weeks
*
**

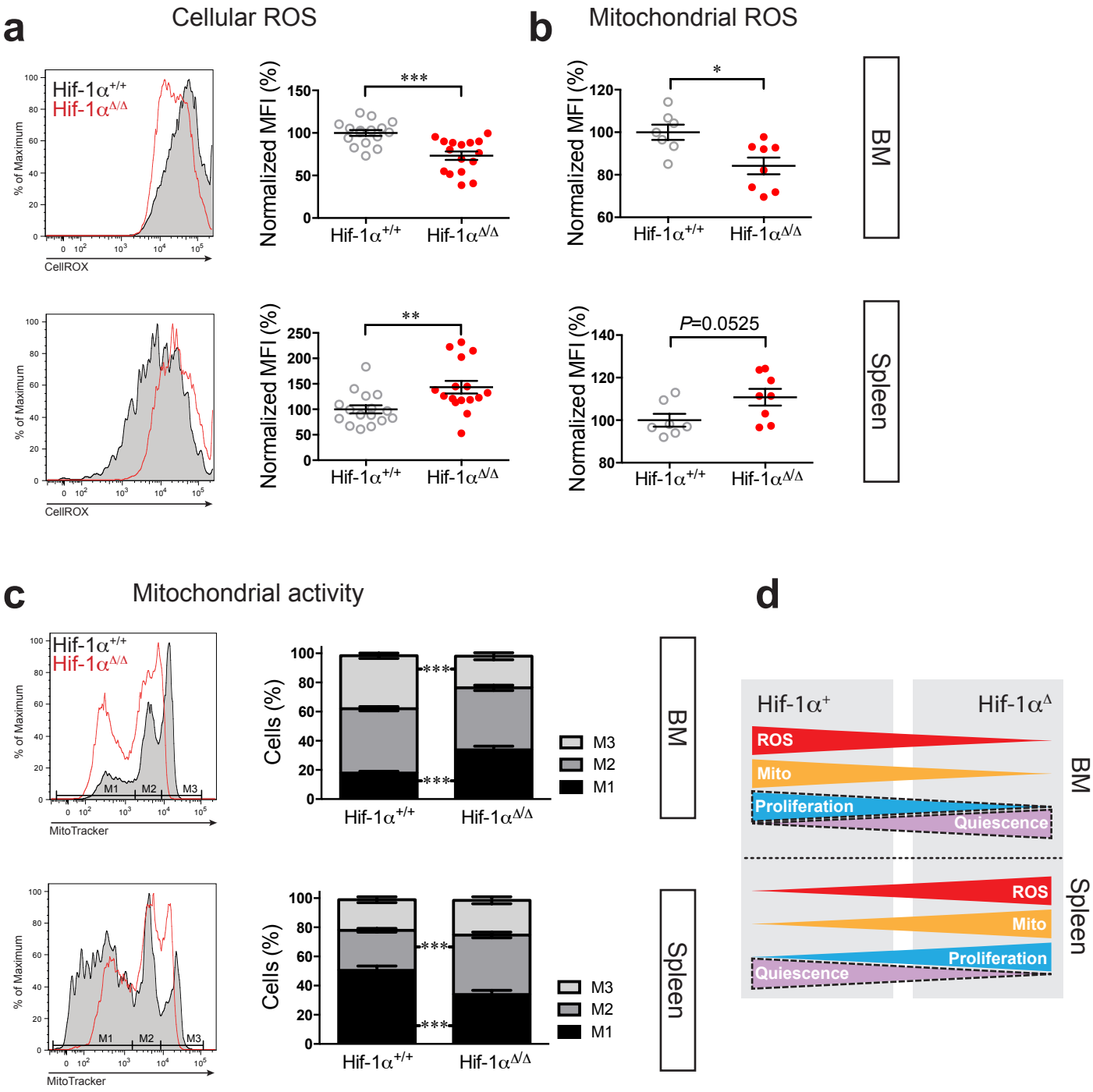
a
Cellular ROS
b
Mitochondrial ROS
Hif-1α+/+
Hif-1αΔ/Δ
% of Maximum
CellROX
Normalized MFI (%)
***
*
**
P=0.0525
BM
Spleen
c
Mitochondrial activity
MitoTracker
M1
M2
M3
Cells (%)
d
Hif-1α+
Hif-1αΔ
ROS
Mito
Proliferation
Quiescence

**Table 1. Peripheral blood counts**

| Parameter | wt mice | *Hif-1*$\alpha^{+/+}$ mice | *Hif-1*$\alpha^{\Delta/\Delta}$ mice | *P*-value (+/Δ) |
|---|---|---|---|---|
| **RBC (x$10^{12}$/L)** | 10.04 ± 0.11 | 9.275 ± 0.19 | 7.707 ± 0.39 | 0.0007 *** |
| **HGB (g/L)** | 148.7 ± 1.59 | 142.8 ± 2.44 | 137.3 ± 3.68 | 0.2069 |
| **HCT** | 0.5158 ± 0.006 | 0.4795 ± 0.009 | 0.4507 ± 0.014 | 0.0835 |
| **Platelets (x$10^{9}$/L)** | 1140 ± 61.11 | 1093 ± 93.76 | 880.0 ± 127.2 | 0.1829 |

RBC: red blood cells; HGB: hemoglobin; HCT: hematocrit. Wt: n=6, *Hif-1*$\alpha^{+/+}$: n=13, *Hif-1*$\alpha^{\Delta/\Delta}$: n=9. Values represent mean ± SEM. *P*-values are calculated between *Hif-1*$\alpha^{+/+}$ and *Hif-1*$\alpha^{\Delta/\Delta}$ groups.

# Supplementary Information

## Loss of HIF-1α accelerates murine FLT-3$^{ITD}$-induced myeloproliferative neoplasia

Talia Velasco-Hernandez[1], Daniel Tornero[2] and Jörg Cammenga[1, 3, 4, 5]

[1]Department of Molecular Medicine and Gene Therapy, Lund Stem Cell Center, Lund University, Lund, Sweden; [2]Laboratory of Stem Cells and Restorative Neurology, Lund Stem Cell Center, Skanes University Hospital, Lund, Sweden; [3]Department of Hematology, Skanes University Hospital, Lund, Sweden, [4]Department of Hematology, Linköping University Hospital and [5]Institution for Clinical and Experimental Medicine, Linköping University, Linköping, Sweden.

Correspondence should be addressed to:

Jörg Cammenga

Department of Molecular Medicine and Gene Therapy

Lund Stem Cell Center BMC A12, Sölvegatan 17, 22184 Lund, Sweden

e-mail: jorg.cammenga@med.lu.se

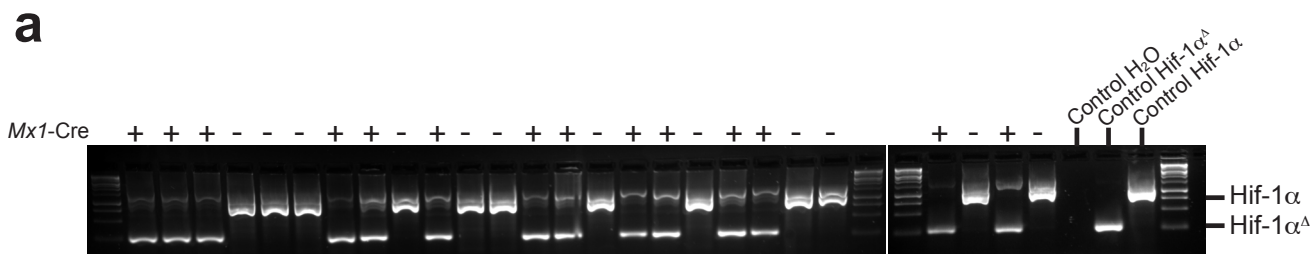


**Supplementary Figure S1. Spontaneous deletion of *Hif-1α.***

(a) Deletion of Hif-1α was checked by PCR amplification of the DNA extracted from BM cells of the mice used in this manuscript. All 14 additionally genotyped mice showed deletion of the HIF-1α gene, providing evidence that spontaneous recombination is a general phenomenon in these mice.

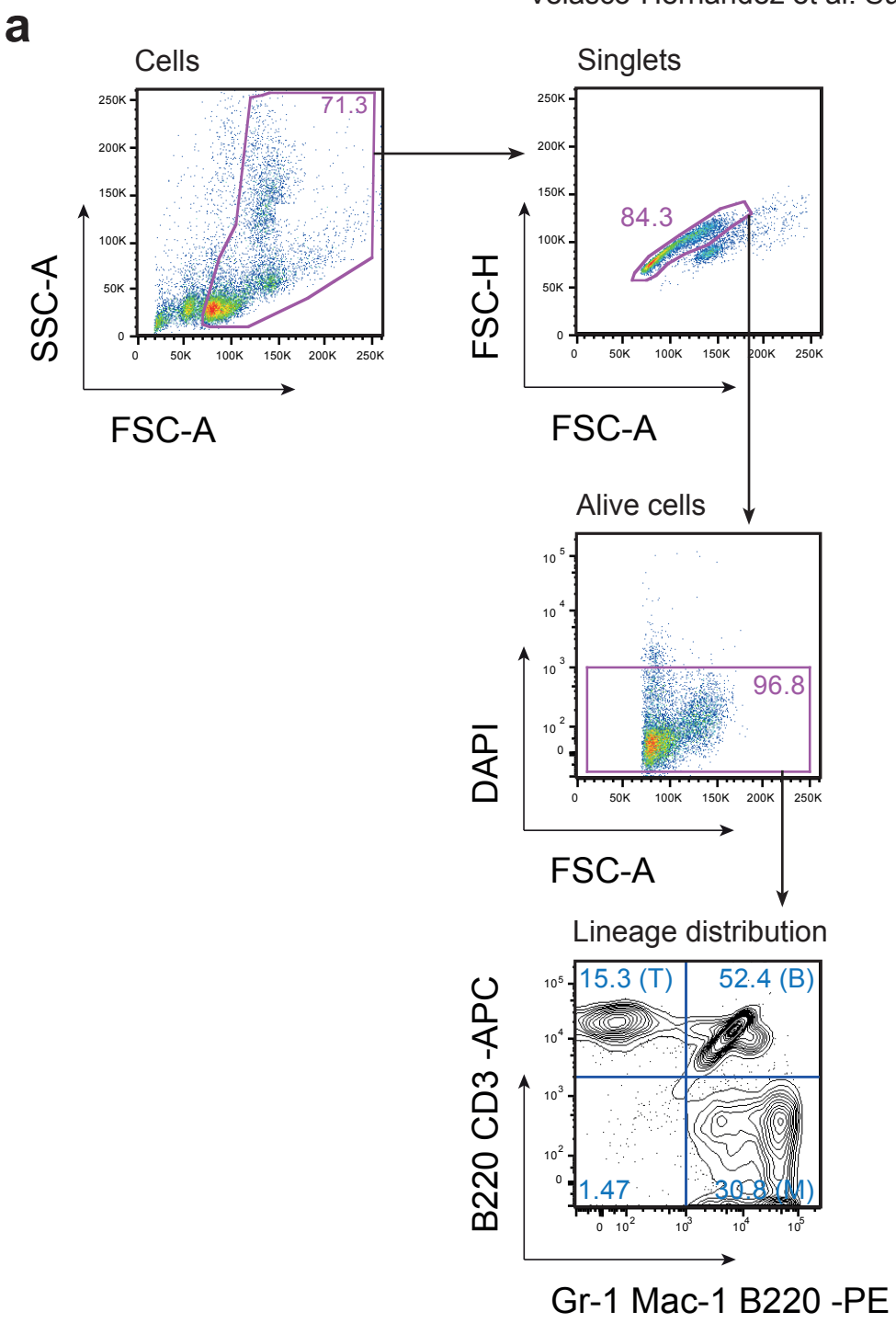


**Supplementary Figure S2. Gating strategy used for the identification of the different cell lineages.**

(**a**) For the identification of the specific lineage populations, we gated entire cells using FSC-A/SSC-A, singlets according to FSC-A/FSC-H, alive cells discarding the DAPI positive cells and finally a combination of Gr1-PE, Mac1-PE, B220-PE, B220-APC and CD3-APC. $PE^+$ cells are myeloid cells (M) ($Gr1^+/Mac1^+$), $PE^+APC^+$ are B cells (B) ($B220^+$) and $APC^+$ are T cells (T) ($CD3^+$).

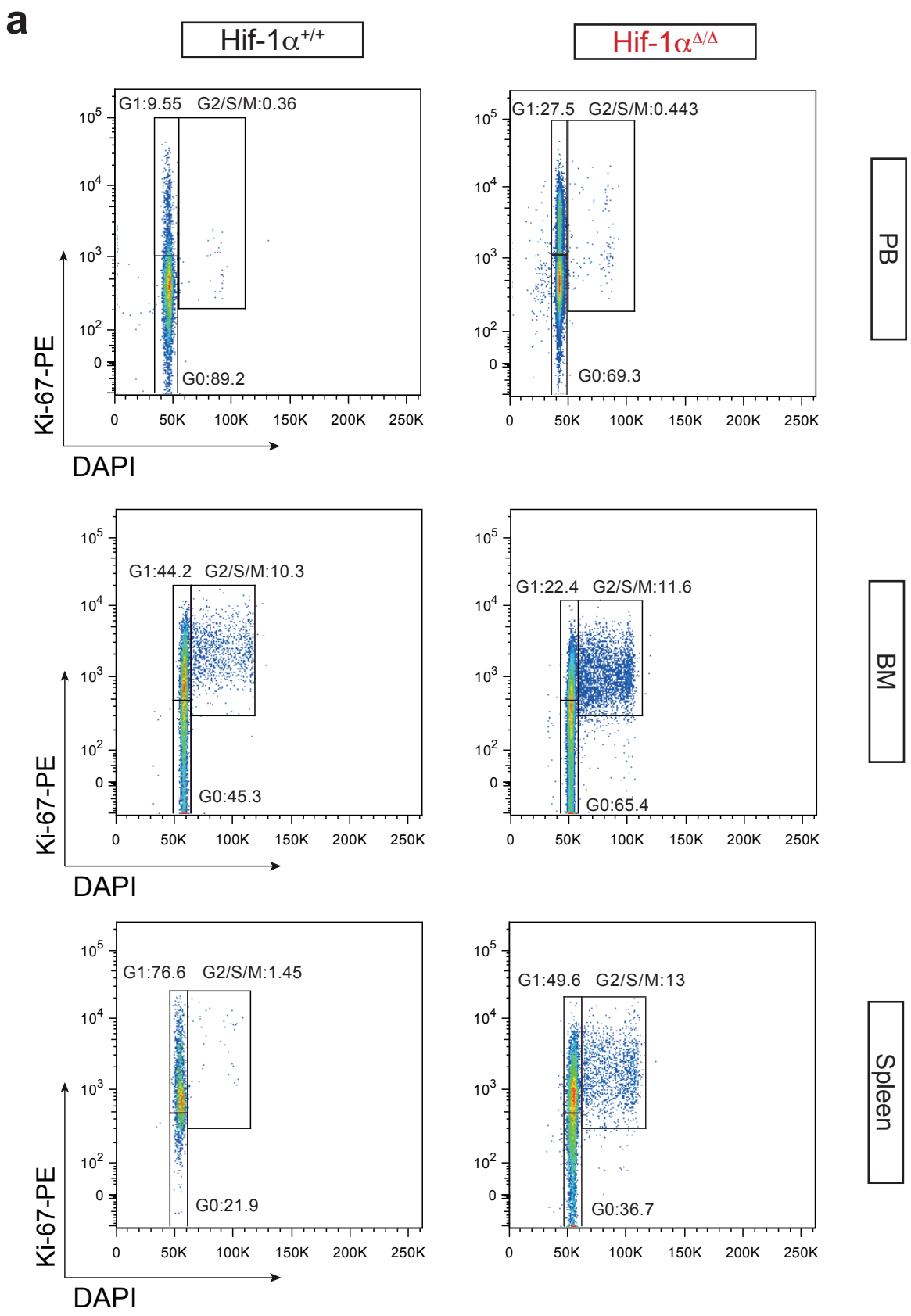


**Supplementary Figure S3. Cell-cycle analysis of myeloid cells.**

(**a**) Representative plots of the cell-cycle analysis of myeloid cells ($Gr1^+/Mac1^+$) located in BM and spleen of HIF-$1\alpha^{\Delta/\Delta}$ and HIF-$1\alpha^{+/+}$ mice .

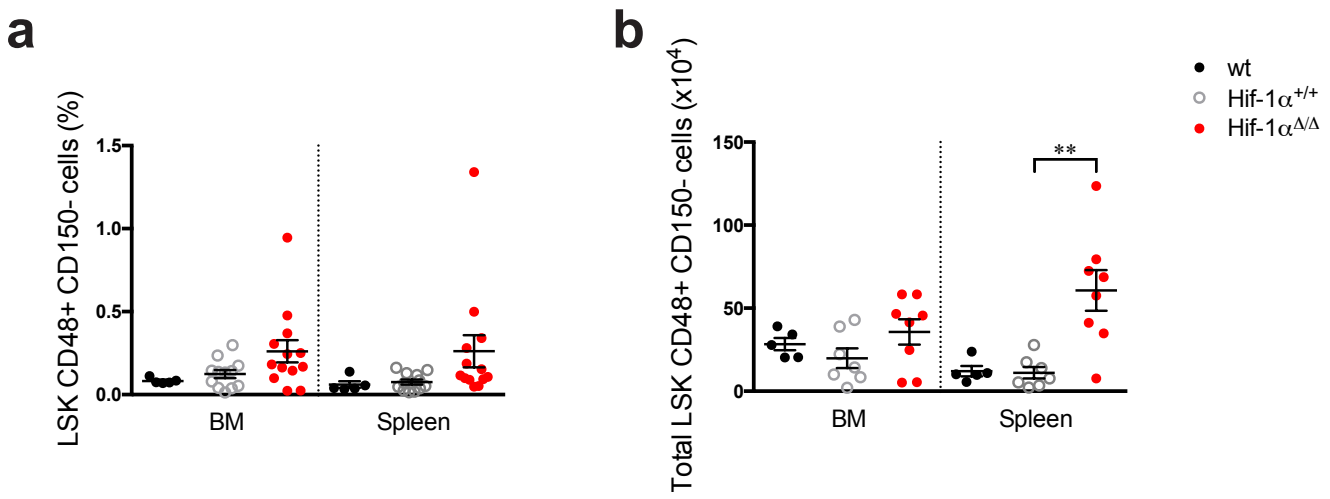


**Supplementary Figure S4. Percentages and total cell numbers of LSK CD48+ CD150- cells in FLT-3$^{ITD}$ mice.**

(**a**) Percentage of LSK CD48+ CD150- cells of total BM or spleen cells (wt, n=5; HIF-1α$^{+/+}$, n=12; HIF-1α$^{Δ/Δ}$, n=13). (**b**) Absolute number of LSK CD48+ CD150- cells in BM (6 bones: 2 femurs, 2 tibiae and 2 hips) or spleen. Plots represent mean ± SEM. Two-tailed Student *t* test was used to assess statistical significance. ***P*<0.01.

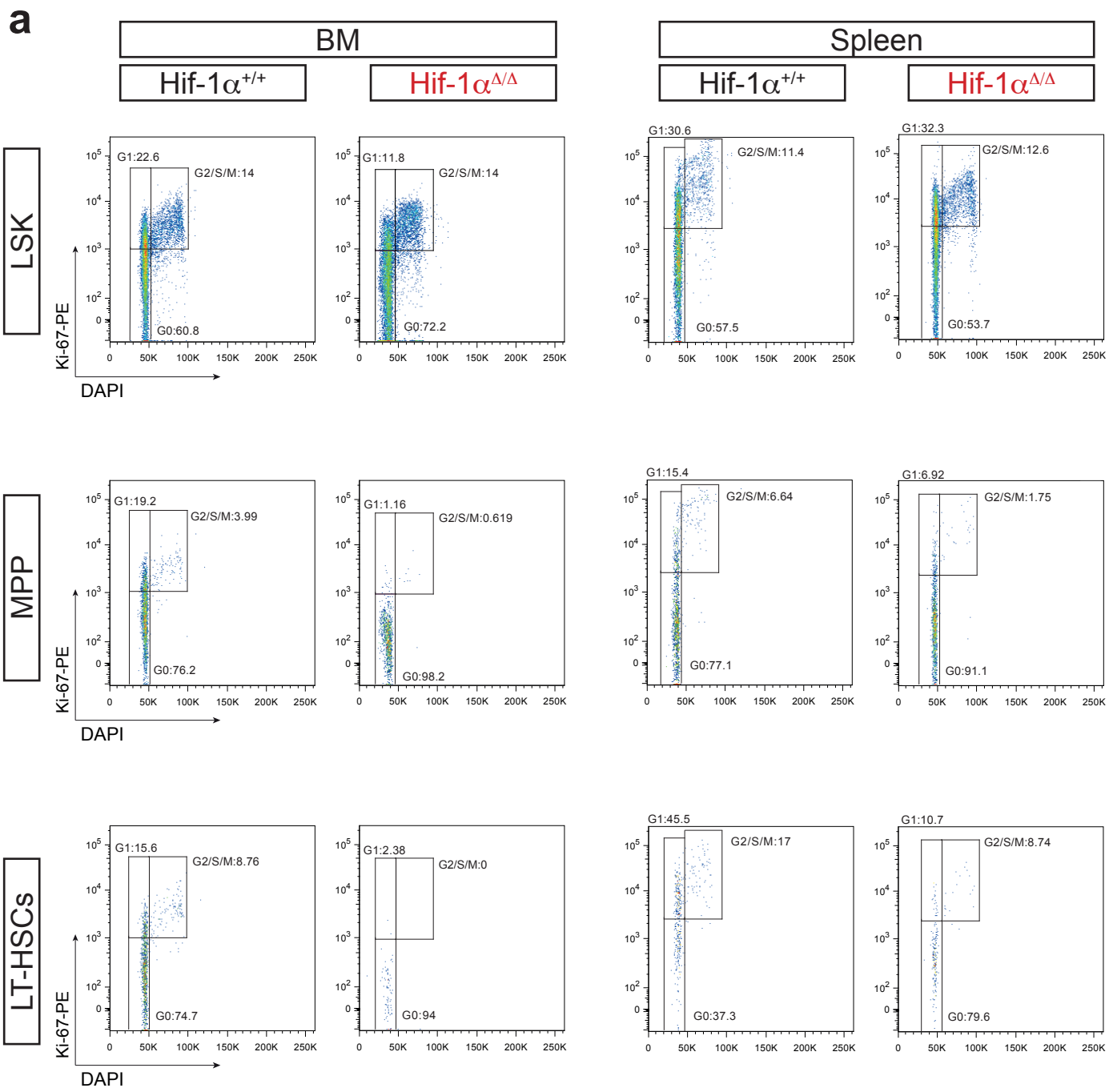


**Supplementary Figure S5. Cell-cycle analysis of primitive populations.**

(**a**) Representative plots of the cell-cycle analysis of the indicated primitive populations located in BM and spleen of HIF-1$\alpha^{\Delta/\Delta}$ and HIF-1$\alpha^{+/+}$ mice .

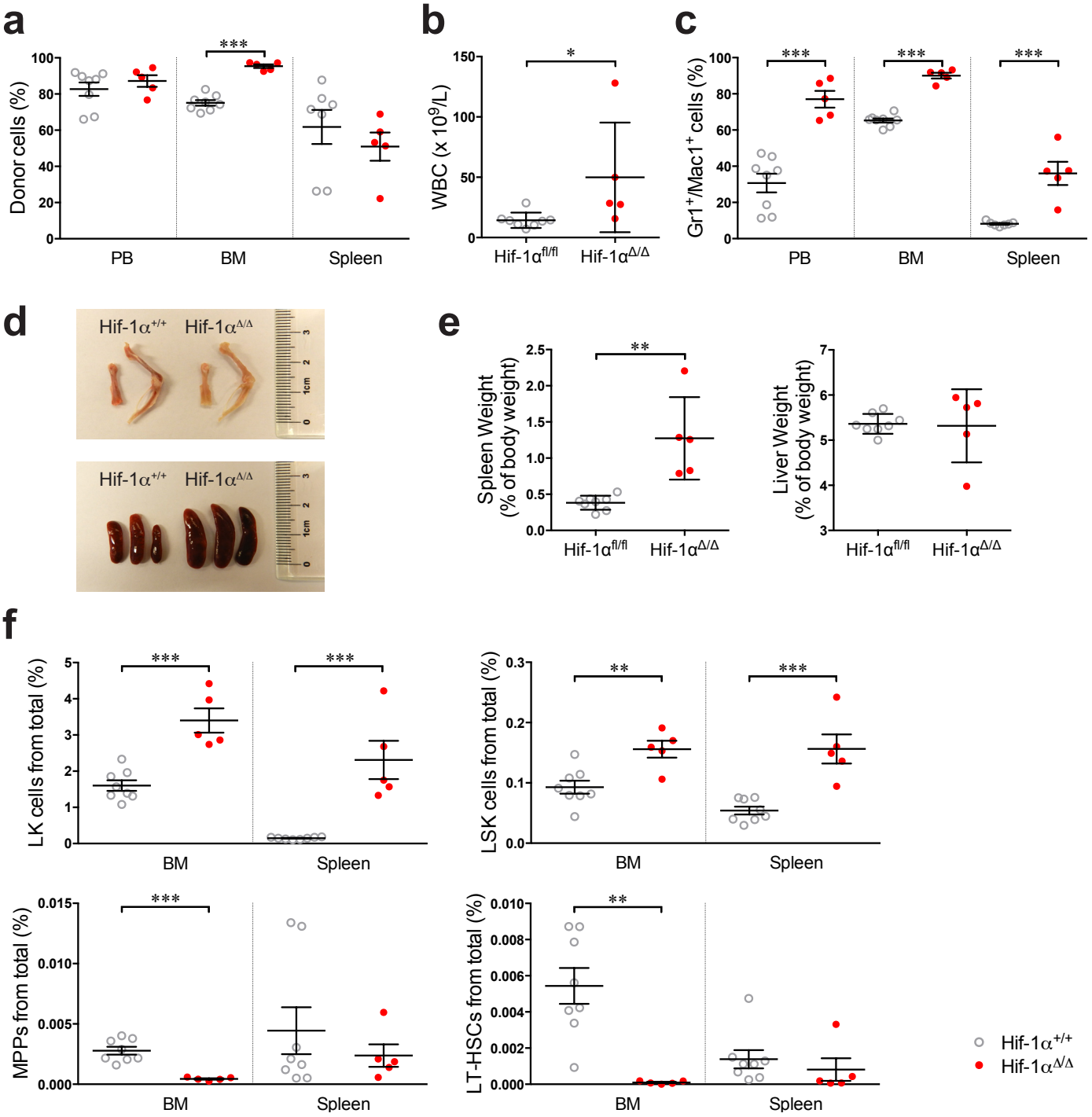


**Supplementary Figure S6. Enhanced FLT-3$^{ITD}$-induced MPN phenotype in mice transplanted with HIF-1α$^{Δ/Δ}$ BM cells.**

(**a**) Donor reconstitution of transplanted mice 47 weeks after transplantation (end point) (n=5-8). (**b**) Blood analysis of mice at the end point, showing increased WBC (n=5-8). (**c**) Percentage of mature myeloid cells (Gr1$^+$/Mac1$^+$) in PB, BM and spleen at the end point (n=5-8). (**d**) Representative phenotype of bones and spleens at the end point from mice with the indicated genotypes. (**e**) Spleen and liver weights in relation to body weight for the different genotypes (n=5-8). (**f**) Percentage of the indicated populations of undifferentiated cells from total BM or spleen cells (n=5-8). Plots represent mean ± SEM. Two-tailed Student *t* test was used to assess statistical significance. **P*<0.05, ***P*<0.01, ****P*<0.001

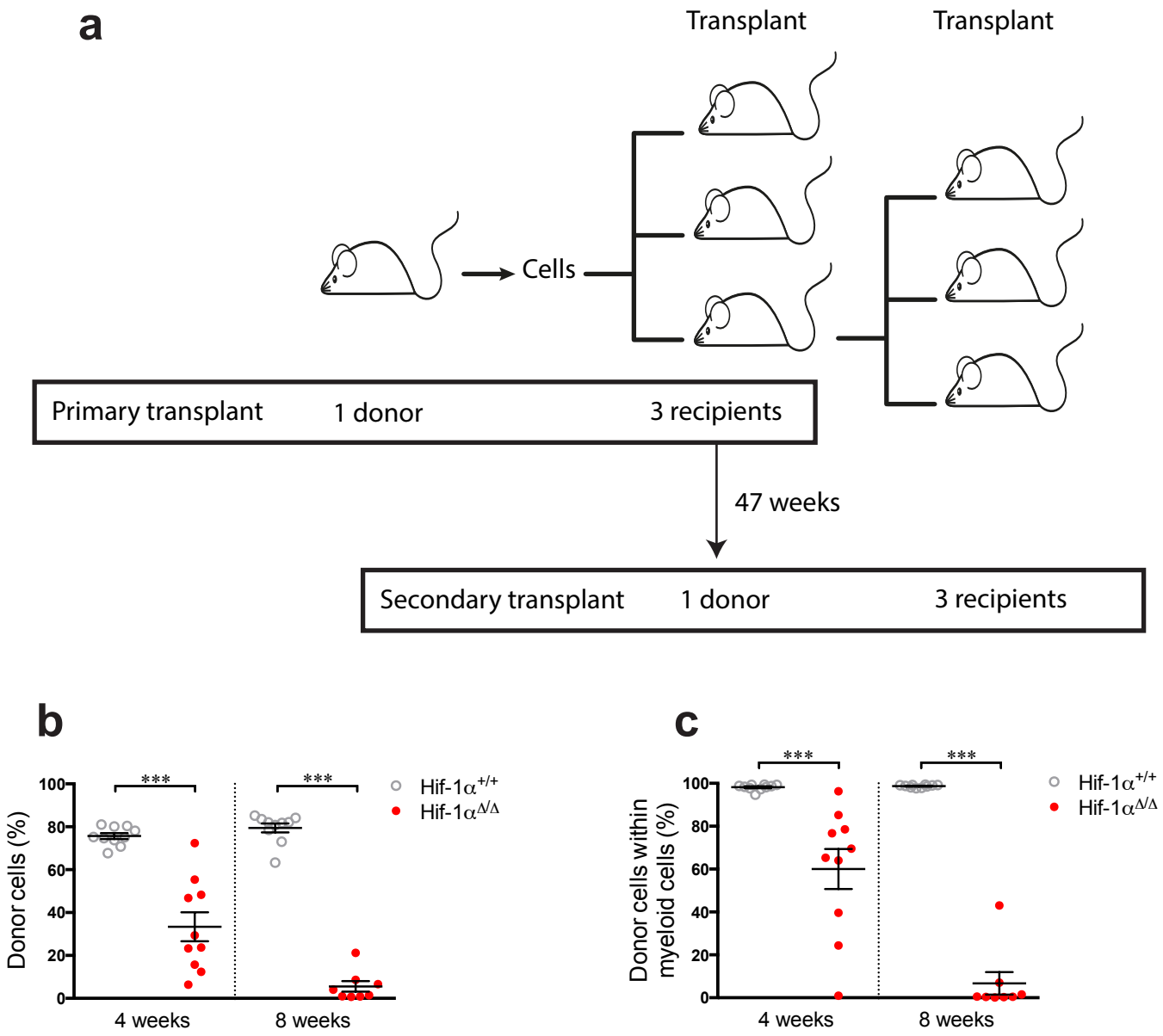


**Supplementary Figure S7. Donor contribution of FLT-3$^{ITD}$ cells in secondary recipients.**

(**a**) Experimental design of the secondary transplantation assay. Donor cells from one primary recipient were transplanted into 3 secondary recipients. Donor cells were harvested 47 weeks after transplantation (end point of the experiment). (**b**) Donor reconstitution of transplanted mice in PB at different time points after transplantation. (n=10) . (**c**) Donor contribution to the myeloid compartment in PB at different time points after transplantation (n=10). Plots represent mean ± SEM. Two-tailed Student *t* test was used to assess statistical significance. ***P<0.001.

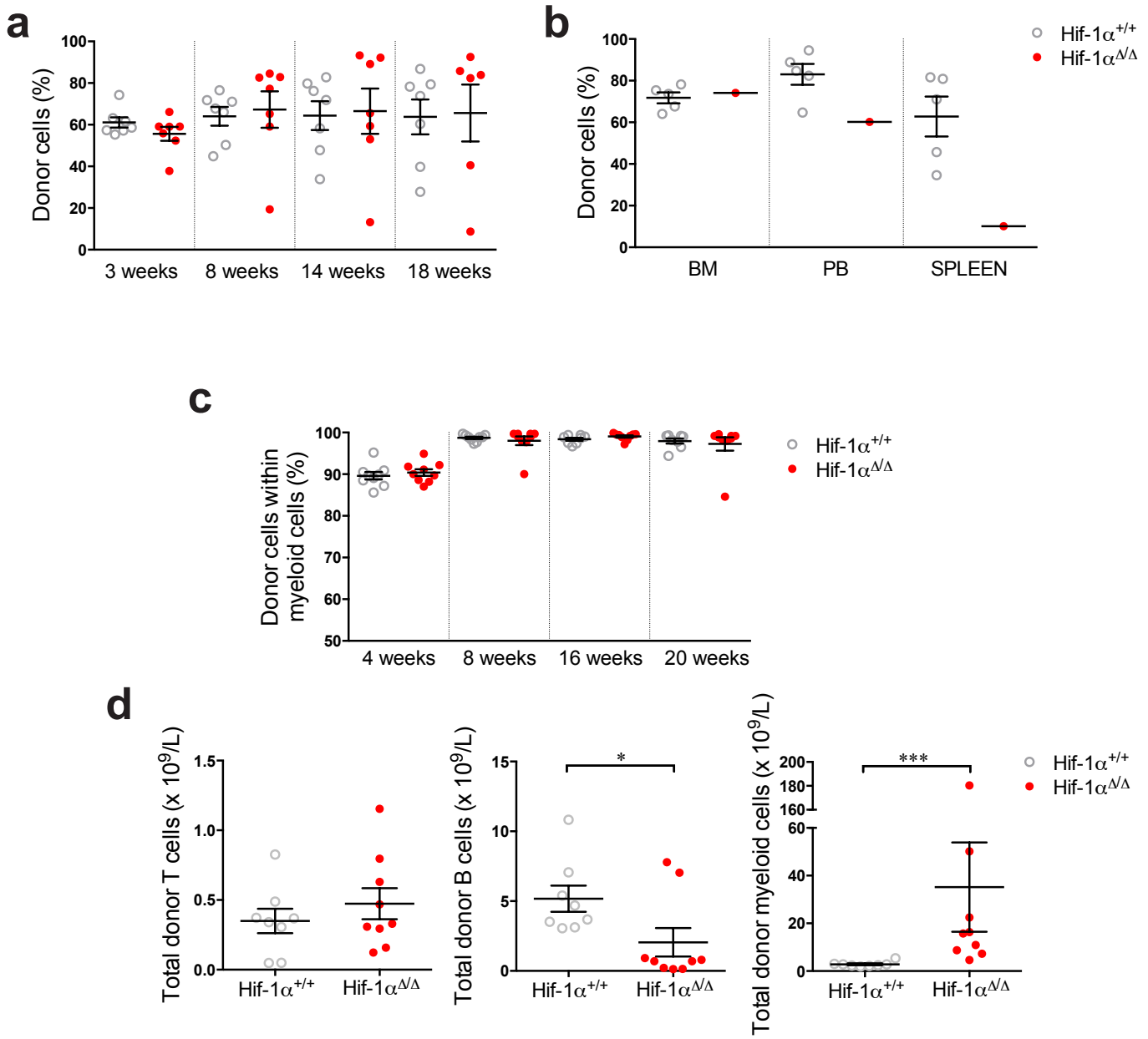


**Supplementary Figure S8. Donor contribution of transplanted FLT-3$^{ITD}$ cells.**

(**a**) Donor contribution of mice transplanted with *in vitro* cultured cells (see also Figure 4b) in PB at different time points after transplantation (n=7) and their donor reconstitution (**b**) in BM, PB and spleen at 62 weeks after transplantation (end point). Notice that at this time point, there is only one HIF-1α$^{Δ/Δ}$ survivor. (**c**) Donor contribution to the myeloid compartment in secondary recipients (see also Figure 4a) at different time points after transplantation cells and (**d**) donor contribution to the different lineages in total cell numbers from the same transplantation at 20 weeks after transplantation. Plots represent mean ± SEM. Two-tailed Student *t* test, and Mann-Whitney test for (d) due to the different variances, were used to assess statistical significance. *P<0.05, ***P<0.001.